Clinical Radiology 74 (2019) 977.e1–977.e7

Contents lists available at ScienceDirect

Clinical Radiology

journal homepage: www.clinicalradiologyonline.net

The value of turbo spin-echo diffusion-weighted imaging apparent diffusion coefficient in the diagnosis of temporal bone cholesteatoma

X. Fan, Z. Liu*, C. Ding, Z. Chang, Q. Ma

Department of Radiology, Shengjing Hospital of China Medical University, Shenyang 110004, China

ARTICLE INFORMATION

Article history:
Received 6 April 2019
Accepted 21 August 2019

AIM: To explore the value of the applying the apparent diffusion coefficient (ADC) to the quantitative diagnosis of temporal bone cholesteatoma.

MATERIALS AND METHODS: Seventy-one patients clinically suspected of temporal bone cholesteatoma were enrolled prospectively. These patients underwent ear magnetic resonance imaging (MRI) and turbo spin-echo diffusion-weighted imaging (TSE-DWI) using a Philips Ingenia 3 T superconductive MRI system, and their ADCs were measured. Subsequently, all enrolled patients underwent surgery within 15 days of the MRI. Using receiver operating characteristic (ROC) curve analysis, the optimal threshold and diagnostic performance for diagnosing temporal bone cholesteatoma were determined. Logistic regression modelling was used to combine ADCs and T1-weighted imaging (T1WI) sequences and calculate the combined diagnostic performance.

RESULTS: Based on the pathology results, patients were categorised into the cholesteatoma group (CS group, n=43) and the non-cholesteatoma group (NCS group, n=28). In the CS group, ADCs were significantly lower (mean, $0.87\pm0.31\times10^{-3}$ mm^2/s) than in the NCS group (mean, $1.87\pm0.49\times10^{-3}$ mm^2/s; $p<0.001$); the area under the ROC curve (AUC) was 0.915. Based on the optimal threshold of ADC, $\leq1.23\times10^{-3}$ mm^2/s, the diagnostic performance was high; the sensitivity and specificity for diagnosing cholesteatoma were 95.35% and 85.71%, respectively. By combining the ADC and T1WI sequence, AUC increased to 0.953, and the sensitivity and specificity were 90.7% and 96.43%, respectively.

CONCLUSION: ADC quantitative analysis has a high value in the preoperative diagnosis of cholesteatoma, and the combination of ADC and T1WI sequences can improve the diagnostic accuracy and specificity and thereby facilitate clinically effective diagnosis.

Introduction

Middle ear cholesteatoma is a disease involving abnormal growth of middle ear keratinised squamous epithelium that is locally invasive, can enhance osteolysis,[1] and can induce conductive hearing impairment, cerebral abscess, and facial paralysis if the lesion expands to invade adjacent structures. Therefore, early diagnosis and surgical treatment of cholesteatoma are of great significance for improving the quality of life. At present, high-resolution computed tomography (HRCT) remains the most common preoperative examination technique for this disease, can clearly display the anatomical structure of the middle ear,

* Guarantor and correspondent: Z. Liu, Department of Radiology, Shengjing Hospital of China Medical University, Shenyang 110004, China.
E-mail address: liuzy@sj-hospital.org (Z. Liu).

https://doi.org/10.1016/j.crad.2019.08.016
0009-9260/

and accurately evaluate the range of cholesteatoma and the degree of temporal bone invasion (e.g., tegmen tympani and ossicular chain); however, it cannot completely diagnose or exclude the presence of cholesteatoma because of fluid aggregation or myxoedema[2] and has low sensitivity and specificity for diagnosing cholesteatoma (≤70%).[3,4]

Cholesteatoma has high keratin content and produces apparently high signals in diffusion-weighted magnetic resonance imaging (DWI). Therefore, head and neck specialists have often used DWI as the common reference method to distinguish cholesteatoma from other middle ear diseases in recent years. Echo planar imaging (EPI) is the most popular DWI technique, but is susceptible to artefacts easily produced by the non-uniform magnetic field of the temporal bone region, and thus has low sensitivity and specificity for diagnosing small-sized cholesteatoma.[4] Non-echo planar imaging (non-EPI) has high spatial resolution and is little influenced by temporal bone artefacts, so can increase the detection rate of small-sized cholesteatoma[5]; however, the diagnostic performance and clinical application value of non-EPI is not consistently recognised.[6–10]

The apparent diffusion coefficient (ADC) reflects the true quantification of water diffusion coefficient per voxel.[11] The diagnostic performance of non-EPI-DWI that relies on qualitative evaluation of cholesteatoma may be surpassed by measuring the ADC value, and thereby, eliminating the diagnostic subjectivity of qualitative imaging and improving diagnostic specificity. Thus, it is more accurate than the subjective qualitative evaluation methods.[12] To date, only a few completed studies have focused on quantitative evaluation of cholesteatoma patients by measuring ADC, and the application of the ADC combined with the T1-weighted imaging (T1WI) sequence to diagnose cholesteatoma has not been reported yet. Therefore, the aim of the present study was to explore the value of applying turbo spin-echo TSE (DWI) sequence-based ADC to the quantitative diagnosis of temporal bone cholesteatoma and the diagnostic value of combining the ADC with the T1WI sequence.

Materials and methods

Patient data

The patients with clinically suspected temporal bone cholesteatoma were prospectively enrolled from January to June 2018. All patients met the following criteria: (1) their ear surgical treatments were not performed before examination; (2) both conventional MRI and TSE-DWI were performed, ADC images were acquired by post-processing, and within the next 15 days the surgical treatment was completed and the histopathological results were obtained. Altogether, 71 patients were enrolled in the study, including 46 males and 25 females, with an age range of 9–72 (mean, 46.44±16.11) years. The study was approved by the ethics committee, and informed consent was obtained from all patients.

Equipment and imaging protocol

The 3 T superconductive MRI system (Ingenia, Philips Electronics Inc., Netherlands), its configured software, and a 32-channel head and neck phased array coil (Invivo Corporation, USA) were used to collect the signals. All patients underwent TSE-DWI and conventional MRI with a scan range from the superior border of the petrous bone to the inferior border of the mastoid process. Axial TSE T1WI and TSE T2WI fat-suppression sequences (3,000 ms repetition time [TR]; 80 ms echo time [TE], 308×192 matrix, 2 mm section thickness, and 1 mm intersection interval) and axial TSE-DWI images (b=0 s/mm^2, 1,000 s/mm^2; 3,000 ms TR, 72 ms TE, 118×87 matrix, 1.5 mm slice thickness, 1 mm intersection interval) were included. The original images were sent to the Intelligence Space Portal workstation (Netherlands), and then ADC images were obtained by post-processing for image evaluation.

Image evaluation

Small-sized cholesteatoma lesions were detected using non-EPI-DWI.[13,14] To measure the ADC of small-sized cholesteatoma (2–3 mm) and detect cholesteatomas within mixed lesions containing both cholesteatoma and inflammatory tissues, a 1 mm^2 circle was selected and marked as the region of interest (ROI) for each lesion separately by two experienced head and neck radiologists. The ROIs were selected to avoid the lesion border (Fig 1); the measurement results from the two radiologists were averaged to obtain the final ADC value, and the final ADCs of lesions were stored in a picture archiving and communication system.

Cholesteatoma was shown as apparently high signals within the middle ear region in the TSE-DWI sequence (b=1000 s/mm^2), but as low signals in the ADC image; T1WI low signal or moderate signal was defined as cholesteatoma. According to the above signal characteristics, T1WI with a low signal or moderate signal was defined as cholesteatoma, whereas T1WI with a high signal was defined as non-cholesteatoma, and two experts, who were both blinded to the clinical data and surgical results of patients, used these definitions to make a uniform diagnosis of either middle ear cholesteatoma or non-cholesteatoma.

Statistical analysis

The continuous variables were expressed as mean ± standard deviation (x±s), analysed with the independent sample *t*-test, and $p<0.05$ indicated a difference that was statistically significant. The histopathological diagnosis was used as the reference standard for the diagnosis of cholesteatoma. Confounding factors were corrected by logistic regression. Using receiver operating characteristic (ROC) curve analysis, the area under the ROC curve (AUC) and 95% confidence interval (95% CI) were calculated: the optimal threshold of diagnosis was determined, and the sensitivity,

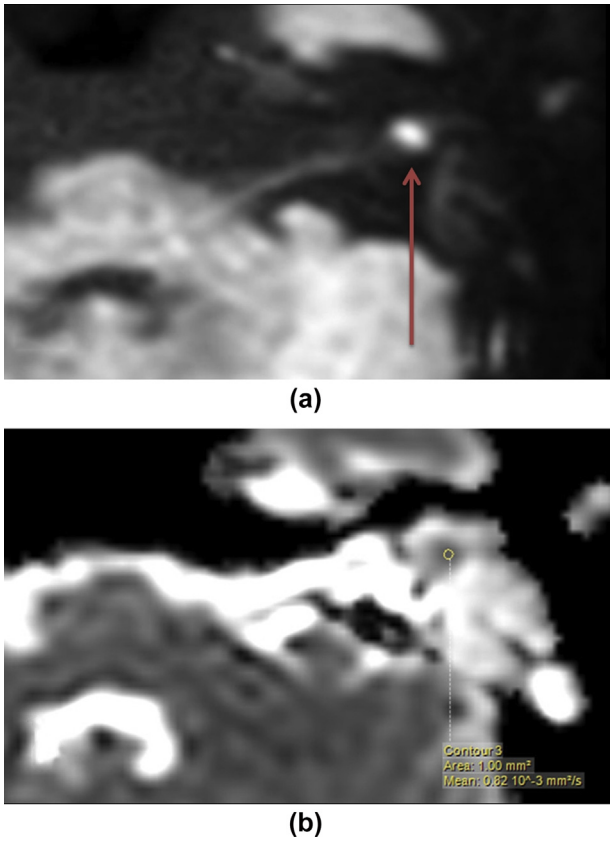

Figure 1 Drawing of the ROI inside the lesion and measuring the ADC. (a) Image from a 3 T MRI scan, axial TSE-DWI sequence (b=1000 s/mm^2). Compared with the adjacent cerebral parenchyma, the lesion in the mastoid process of left middle ear displayed high signals (red arrow). (b) In the ADC image, a 1 mm^2 ROI was marked within the internal border of lesion (yellow circle), and the mean ADC was 0.82×10^{-3} mm^2/s.

specificity, positive predictive value, and negative predictive value were computed to evaluate the diagnostic performance of the ADC. The ADC was combined with the T1WI sequence by logistic regression analysis, and then the diagnostic accuracy, sensitivity, and specificity of such combinations for cholesteatoma were calculated and compared. All data were analysed using SPSS version 17.0 (SPSS, Chicago, IL, USA) and MedCalc (version 15.2.2, Ostend, Belgium) statistical software.

Results

Patient characteristics

All 71 patients with clinically suspected temporal bone cholesteatoma underwent surgical treatment and histopathological examination. They were then categorised into the cholesteatoma group (CS group, n=43) and the non-cholesteatoma group (NCS group n=28) according to the postoperative histopathology results. The demographic and symptomatic characteristics are shown in Table 1. The mean length of lesions in the CS group was 9±3.9 mm (range, 3–20 mm).

Table 1
Demographic characteristics and initial symptoms by study group (n=71).

Variable	n	%	CS group	NCS group	p-Value
Sex					0.617
Male	46	64.79%	29 (40.85%)	17 (23.94%)	
Female	25	35.21%	14 (19.72%)	11 (15.49%)	
Age			42.37±17.66	52.67±11.4	0.004
Primary clinical manifestations					
Otopyorrhoea	64	90.14%	40 (56.34%)	24 (33.8%)	0.422
Perforation	46	64.79%	26 (36.62%)	20 (28.17%)	0.448
Facial numbness	6	8.45%	4 (5.63%)	2 (2.82%)	1.000

CS, cholesteatoma group; NCS, non-cholesteatoma group.

Comparison of ADCs between the CS and NCS groups

The ADCs of the CS group were significantly lower than those of the NCS group mean, $0.87\pm0.31\times10^{-3}$ mm^2/s (range, 0.41×10^{-3}–2.26×10^{-3} mm^2/s) versus mean, $1.87\pm0.49\times10^{-3}$ mm^2/s (range 0.59×10^{-3}–2.39×10^{-3} mm^2/s; $p<0.05$; Figs. 2a–g,3). The optimal threshold of ADC for cholesteatoma diagnosis was determined by ROC curve analysis. The largest AUC (AUC=0.915) was observed using the ADC threshold of $\leq1.23\times10^{-3}$ mm^2/s (Fig 4). Based on this threshold, the sensitivity, specificity, positive predictive value, and negative predictive value for diagnosing temporal bone cholesteatoma were 95.35%, 85.71%, 91.11%, and 92.11%, respectively. Four cases were falsely positive, including two cases of mastoid abscess and two cases of cholesterol crystals. Two cases were falsely negative; both had infiltration of numerous inflammatory cells and the formation of granulation tissues enclosing a small squamous epithelium area of tissue liner (Fig. 2i–l).

Comparison of ADC between various NCS subgroups and CS group found no significant difference in ADC between the mastoid abscess subgroup (mean, $0.63\pm0.18\times10^{-3}$ mm^2/s) or the cholesterol crystal subgroup (mean, $1.05\pm0.06\times10^{-3}$ mm^2/s) and the CS group (mean, $0.87\pm0.31\times10^{-3}$ mm^2/s) and found a significant difference between the other subgroups and the CS group (Table 2).

Diagnosis of cholesteatoma using combined ADC and T1WI images

In the CS group, T1WI of 41 patients yielded low signals or moderate signals and T1WI of two patients produced high signals. In the NCS group, T1WI of 21 patients yielded low signals or moderate signals and T1WI of seven patients yielded high signals. T1WI was of statistical significance for the diagnosis of cholesteatoma and non-cholesteatoma (p=0.024; Table 3), and the sensitivity and specificity were 95.35% and 25%.

After combining T1WI sequences and ADCs, logistic regression analysis was performed to obtain the combined ROC curve; AUC for the combination (AUC=0.953) was significantly higher than that for the ADC alone (AUC=0.915; p=0.0378; Fig 5). The sensitivity and specificity of this combination for diagnosing cholesteatoma were 90.7% and 96.43%, respectively. Two cases were falsely positive (mastoid abscess).

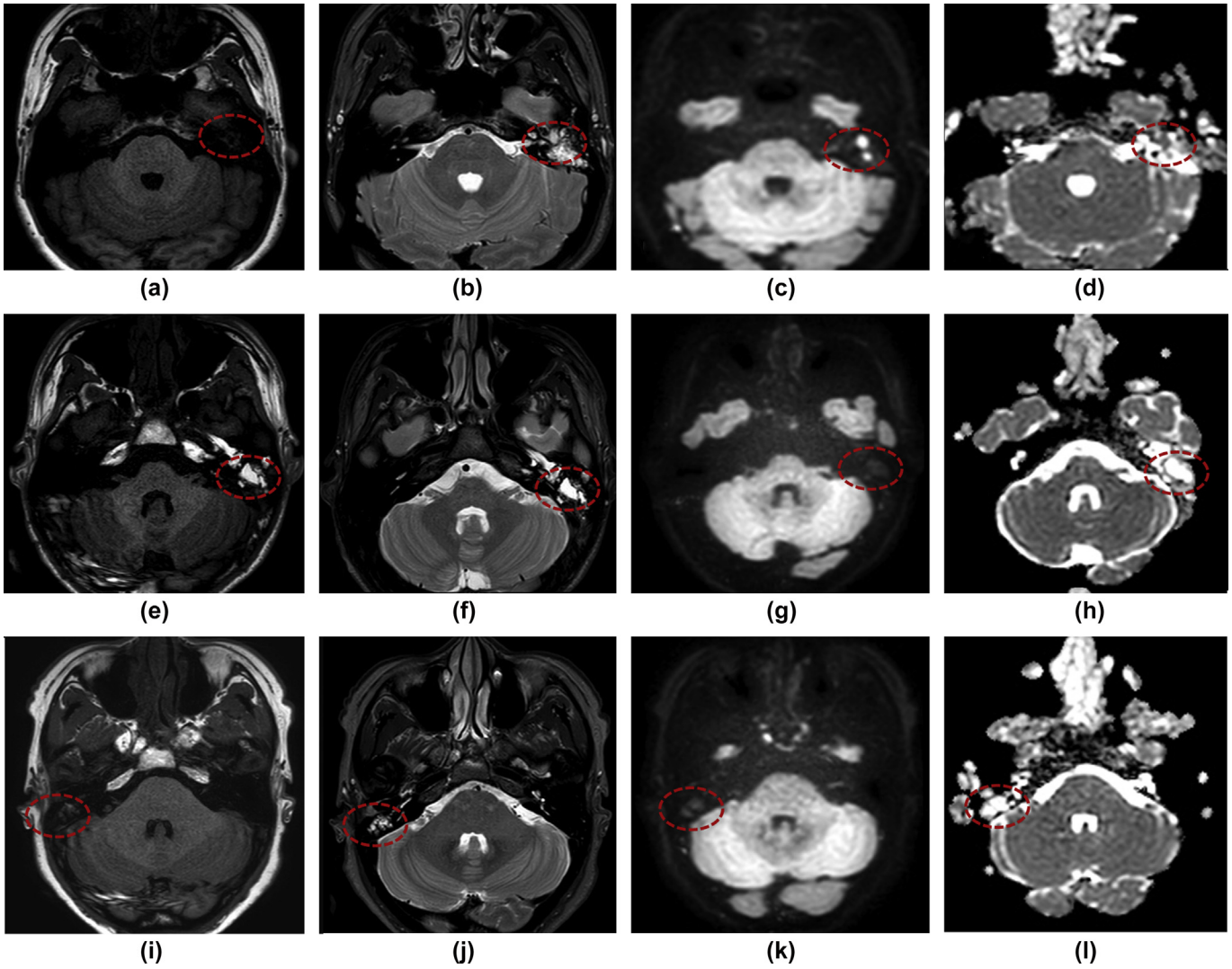

Figure 2 (a–d) MRI images of a histopathologically diagnosed cholesteatoma. (a) Low signals are observed in the axial T1WI image (red oval). (b) Non-uniform, high signals are observed in the T2WI image with an unclear border (red oval). (c) Limited diffusion and apparently high signals (red oval) are observed in the axial TSE-DWI image (b=1000 s/mm^2), with a clear border. (d) Low signals are observed in the ADC image (red oval): the ADC of the lesion measures 0.78×10^{-3} mm^2/s; (e–h) DWI qualitative analysis of surgically confirmed lesions with fibrous tissues, calcification, and old haemorrhage. (e) High signals are observed in the axial T1WI image (red oval). (f) Coronal T2-weighted image demonstrates a well-defined lesion (red oval) in the left mastoid. (g) The lesion (red oval) has low signal intensity on TSE-DWI images (b=1000 s/mm^2) that is not higher than brain tissue (oval), and demonstrates high signal intensity (red oval; h). The ADC of the lesion measures 2.31×10^{-3} mm^2/s; (i–l) Coronal images of a false-negative case for detection of non-cholesteatoma in the right mastoid using the qualitative method. (i) Moderate signals are observed in the axial T1WI image (red oval). (j) High signals are observed in the T2WI image with an unclear border (red oval). (k) TSE-DWI images (b=1000 s/mm^2) show slightly low signal intensity relative to brain tissue. (l) The ADC map shows high signal intensity (red oval). The ADC of the lesion measures 1.5×10^{-3} mm^2/s.

Discussion

ADC quantitative analysis is a useful diagnostic indicator to more accurately diagnose temporal bone cholesteatoma, and the combination of the ADC map and T1WI sequence can improve diagnostic accuracy. A major strength of this study was confirming the diagnoses all patients (including non-cholesteatoma patients) by surgical histopathology.

The mean ADC in the CS group was remarkably and significantly lower than that in the NCS group. These findings are consistently supported by previously reported results.[15,16] The significant difference in signals between the two groups is primarily attributable to the composition of the cholesteatoma that restricted water diffusion and is displayed as apparently high signals in TSE-DWI but low signals in ADC images. In contrast, most non-cholesteatoma lesions contain inflammatory granulation tissue and fibrosis that display low signals in DWI.[17] In this study, the mean ADC in the CS group was $0.87\pm0.31\times10^{-3}$ mm^2/s, slightly lower than the result ($1\pm0.1\times10^{-3}$ mm^2/s) previously reported by Ozgen *et al.*[15] Such a difference may be related to how ROIs were selected: Ozgen *et al.*[15] marked a ROI of 3

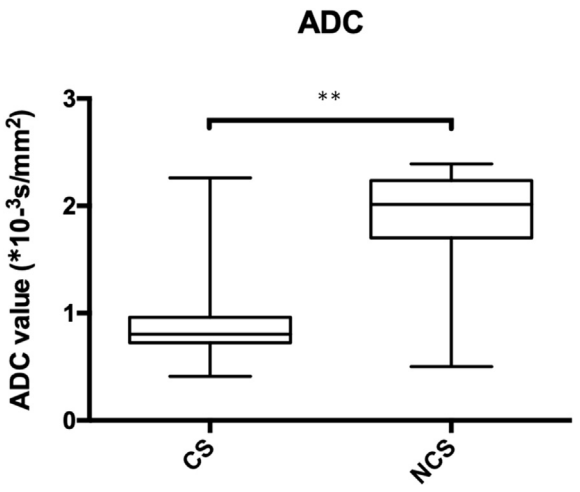

Figure 3 Boxplots comparing distribution of ADC values in the CS and NCS groups. Range of the CS group (0.41×10^{-3}–2.26×10^{-3} mm^2/s); Range of the NCS group (0.59×10^{-3}–2.39×10^{-3} mm^2/s). $^{**}p<0.05$. CS, cholesteatoma group; NCS, non-cholesteatoma group.

mm^2, whereas the ROIs in this study were 1 mm^2, more precise than a 3 mm^2 ROI. The 1 mm^2 ROI enabled detection of small-sized cholesteatomas within mixed lesions containing both cholesteatoma and inflammatory tissues and thus avoided the interference of inflammatory tissues at the border of lesions, so ADCs were of slightly lower value. In addition, this difference may have been due to the use of 3 T MRI in the present study for image acquisition with a higher signal-to-noise ratio (SNR) that supports better visualisation of lesions; thus, the ADC is measured more accurately. In the present study, the ADC ranged from 0.41×10^{-3}–2.26×10^{-3} mm^2/s in the CS group and from 0.5×10^{-3}–2.39×10^{-3} mm^2/s in the NCS group, so the values overlapped between the two groups; however, Russo *et al.*[16] found no overlapping of the range of ADC values in CS and NCS groups. Perhaps this was because they did not include mastoid abscess patients. In contrast, the present study

Table 2
Comparison of apparent diffusion coefficients (ADCs) between NCS subgroups and the CS group (n=28).

NCS subgroup	n	%	ADC mean ($\times10^{-3}$ mm^2/s)	p-Value[a]
Granulation tissues	7	25%	2.13±0.09	0.0006
Effusion	2	7.143%	2.11±0.24	0.0002
Abscess	2	7.143%	0.63±0.18	0.306
Neurilemmoma	2	7.143%	1.5±0.11	0.008
Fibrous tissues	3	10.714%	1.98±0.26	0.0004
Fibrous tissues with calcification and old haemorrhage	5	17.857%	2±0.28	0.0009
Tympanic polyp	3	10.714%	2.15±0.22	0.0001
Cholesterol crystal	2	7.143%	1.05±0.06	0.421
Aspergillus cenobium	2	7.143%	2.3±0.11	0.0001

In the CS group, mean ADC was $0.87\pm0.31\times10^{-3}$ mm^2/s.
CS, cholesteatoma group; NCS, non-cholesteatoma group.
[a] Compared with the CS group.

Table 3
T1-weighted imaging (WI) images and surgical pathology results.

	CS group	NCS group	Total
T1WI low signals or moderate signals	41	21	62
T1WI high signals	2	7	9
Total	43	28	71

CS, cholesteatoma group; NCS, non-cholesteatoma group.

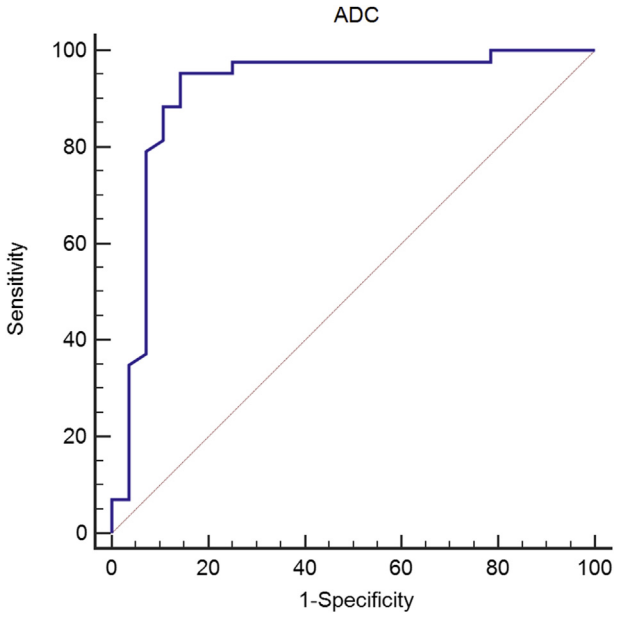

Figure 4 ROC curve (blue line) of ADC values for diagnosis of cholesteatoma using data from the CS group and the NCS group.

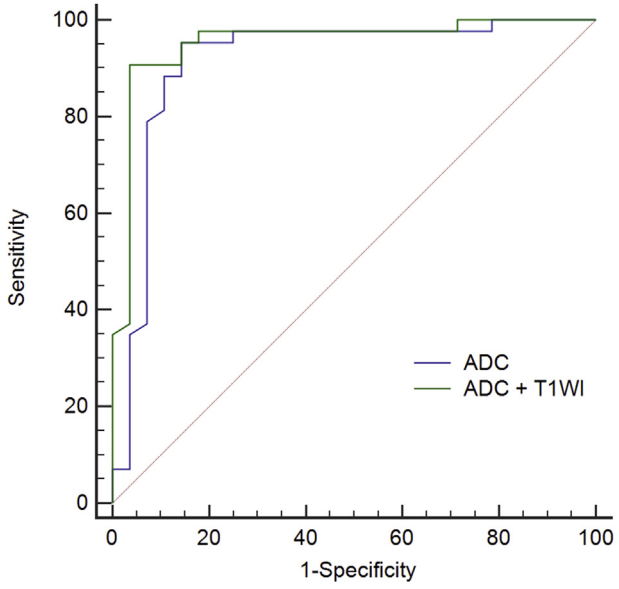

Figure 5 Comparison of the diagnostic performance (ROC curve analysis) between the combination of the ADC and T1WI sequence and the ADC alone. The AUC of the combination of the ADC and T1WI sequence (ADC+T1WI) was significantly greater than that of the ADC alone ($p<0.05$).

included two patients who were diagnosed pathologically with mastoid abscess, and the mean ADC in the mastoid abscess subgroup was lower than that in the CS group ($0.63\pm0.18\times10^{-3}$ versus $0.87\pm0.31\times10^{-3}$ mm^2/s), thus contributing to the overlapping of ADCs in the CS and NCS groups.

This study demonstrated that when the optimal threshold of ADC, $\leq1.23\times10^{-3}$ mm^2/s, was used to diagnose temporal cholesteatoma the sensitivity and specificity were 95.35% and 85.71%, respectively; these are nearly identical to the conclusions of previous studies.[12,15] The optimal threshold of ADC (value with greatest diagnostic performance) in the study of Lingam[12] *et al.* was 1.30×10^{-3} and 1.24×10^{-3} mm^2/s in the study of Özgen.[15] In the present study, at the optimal threshold of ADC, the AUC (0.915) was lower than that (AUC=0.97) in the study of Lingam.[12] It may be because MRI-negative patients in the study of Lingam[12] only underwent otoscopy or conventional follow-up, but lacked surgical treatment and pathological results. Four of the present cases were false positives, including two cases of cholesterol crystal and two cases of mastoid abscess. Cholesterol crystals can be identified by combining the ADC with T1WI. Cholesterol granuloma is displayed as high signal at T1WI, which helps to differentiate cholesteatoma from cholesterol granuloma.[18] Furthermore, Fukuda *et al.*[19] concluded that combining the ADC with the T1WI sequence could improve the diagnostic specificity for cholesteatoma by excluding some false-positive cases. Of note, mastoid abscess is quite limited in diffusion, and its ADC is far lower than that of cholesteatoma lesions.[20] The studies have shown that ADC can be used to distinguish cholesteatoma and abscess. In the present study, ADCs did not differ significantly between mastoid abscess patients and cholesteatoma patients (mean, $0.63\pm0.18\times10^{-3}$ versus $0.87\pm0.31\times10^{-3}mm^2/s$), which differs from the study conclusion of Karandikar *et al.*[20]; this difference may be related to the small number of mastoid abscess patients in the present study. Mastoid abscess has a rapid onset and distinctive clinical symptoms; and Nash *et al.*[9] believed that non-EPI-DWI was a supplement to clinical judgment and to comprehensively diagnose cholesteatoma, it was important to combine the clinical symptoms and medical history. In addition, there were two false-negative cases in the present study, which were attributed to the infiltration of numerous inflammatory cells and the formation of granulation tissues enclosing a small squamous epithelium area of tissue liner. The signals of inflammatory granuloma and cholesteatoma overlapped, which increased the actual ADC of such lesions.

Cholesteatoma lesions are displayed as low signals or moderate signals in T1WI, while cholesterol granulomas are shown as high signals in T1WI; thus, T1WI can be used to distinguish cholesterol granuloma lesions.[18] Therefore, the evaluation criteria for cholesteatoma of high signals in DWI and moderate signals or low signals in T1WI was adopted to decrease the false-positive rate in some evaluations of temporal bone cholesteatoma with non-EPI-DWI.[19] The present study showed that T1WI sequence had an interesting diagnostic value for cholesteatoma; its sensitivity and specificity were 95.35% and 25%, respectively. After T1WI was combined with the ADC, the diagnostic accuracy (AUC=0.953) was significantly greater than that of the ADC alone (AUC=0.915; $p<0.05$). In evaluating cholesteatoma lesions, the sensitivity and specificity of ADC alone were 95.35% and 85.71%, respectively, and four cases were falsely positive cases; they were 90.7% and 96.43%, respectively, when the T1WI sequence was combined with the ADC, and only two cases of mastoid abscess were falsely positive. This suggests that ADC quantitative analysis has high diagnostic performance for evaluating temporal bone cholesteatoma, and its combination with T1WI can improve the diagnostic accuracy and reduce the false-positive rate.

The present study has some shortcomings. Firstly, the present study demonstrated that cholesteatoma and non-cholesteatoma patients had significantly different ages, which may be related with an unbalance of study samples, fewer non-cholesteatoma cases than cholesteatoma cases, and a small simple size. Secondly, the ADC value of lesions was associated with the ROI marked by the observer, thus measurement bias is unavoidable. Finally, the present study has a small sample size and lacks small-sized lesions (diameter <3 mm), so the further studies with a larger sample size are still needed.

In summary, ADC quantitative analysis can help to distinguish cholesteatoma and non-cholesteatoma lesions. The ADC value, when considered along with the clinical history and conventional sequence (T1WI) examination can improve diagnostic accuracy, so it is valuable for diagnosing temporal bone cholesteatoma.

Conflict of interest

We declare that we have no financial and personal relationships with other people or organizations that can inappropriately influence our work, there is no professional or other personal interest of any nature or kind in any product, service and/or company that could be construed as influencing the position presented in, or the review of, the manuscript entitled.

References

1. Kuo C-L. Etiopathogenesis of acquired cholesteatoma: prominent theories and recent advances in biomolecular research. *The Laryngoscope* 2015;**125**(1):234–40. https://doi.org/10.1002/lary.24890.
2. Mas-Estelles F, Mateos-Fernandez M, Carrascosa-Bisquert B, *et al.* Contemporary non-echo-planar diffusion-weighted imaging of middle ear cholesteatomas. *RadioGraphics* 2012;**32**(4):1197–213. https://doi.org/10.1148/rg.324115109.
3. Yigiter AC, Pinar E, Imre A, *et al.* Value of echo-planar diffusion-weighted magnetic resonance imaging for detecting tympanomastoid cholesteatoma. *J Int Adv Otol* 2015;**11**(1):53–7. https://doi.org/10.5152/iao.2015.447.
4. Songu M, Altay C, Onal K, *et al.* Correlation of computed tomography, echo-planar diffusion-weighted magnetic resonance imaging and surgical outcomes in middle ear cholesteatoma. *Acta Otolaryngol* 2015;**135**(8):776–80. https://doi.org/10.3109/00016489.2015.1021931.
5. van Egmond SL, Stegeman I, Grolman W, *et al.* A systematic review of non-echo planar diffusion-weighted magnetic resonance imaging for detection of primary and postoperative cholesteatoma. *Otolaryngol Head Neck Surg* 2015;**154**(2):233–40. https://doi.org/10.1177/0194599815613073.

6. von Kalle T, Amrhein P, Koitschev A. Non-echoplanar diffusion-weighted MRI in children and adolescents with cholesteatoma: reliability and pitfalls in comparison to middle ear surgery. *Pediatr Radiol* 2015;**45**(7):1031–8. https://doi.org/10.1007/s00247-015-3287-y.
7. Garrido LCC, Montoya J, Alonso A, *et al*. Diagnostic capacity of non-echo planar diffusion-weighted MRI in the detection of primary and recurrent cholesteatoma. *Acta Otorrinolaringol Esp* 2015;**66**(4):199–204. https://doi.org/10.1016/j.otorri.2014.07.006.
8. Lingam RK, Bassett P. A meta-analysis on the diagnostic performance of non-echoplanar diffusion-weighted imaging in detecting middle ear cholesteatoma. *Otol Neurotol* 2017;**38**(4):521–8. https://doi.org/10.1097/mao.0000000000001353.
9. Nash R, Lingam RK, Chandrasekharan D, *et al*. Does non-echo-planar diffusion-weighted magnetic resonance imaging have a role in assisting the clinical diagnosis of cholesteatoma in selected cases? *J Laryngol Otol* 2018;**132**(03):207–13. https://doi.org/10.1017/s0022215118000087.
10. Clarke SE, Mistry D, AlThubaiti T, *et al*. Diffusion-weighted magnetic resonance imaging of cholesteatoma using PROPELLER at 1.5 T: a single-centre retrospective study. *Can Assoc Radiol J* 2017;**68**(2):116–21. https://doi.org/10.1016/j.carj.2016.05.002.
11. Le Bihan DBE, Lallemand D, Aubin ML, *et al*. Separation of diffusion and perfusion in intravoxel incoherent motion MR imaging. *Radiology* 1988;**168**(2):497–505. https://doi.org/10.1148/radiology.168.2.3393671.
12. Lingam RKKP, Hughes J, Singh A. Apparent diffusion coefficients for detection of postoperative middle ear cholesteatoma on non-echo-planar diffusion-weighted images. *Radiology* 2013;**269**(2):504–10. https://doi.org/10.1148/radiol.13130065.
13. Migirov LWM, Greenberg G, Eyal A. Non-EPI DW MRI in planning the surgical approach to primary and recurrent cholesteatoma. *Otol Neurotol* 2014;**35**(1):121–5. https://doi.org/10.1097/MAO.0000000000000234.
14. Garcia-Iza L, Guisasola A, Ugarte A, *et al*. Utility of diffusion-weighted magnetic resonance imaging in the diagnosis of cholesteatoma and the influence of the learning curve. *Eur Arch Otorhinolaryngol* 2018;**275**(9):2227–35. https://doi.org/10.1007/s00405-018-5074-5.
15. Özgen B, Bulut E, Dolgun A, *et al*. Accuracy of turbo spin-echo diffusion-weighted imaging signal intensity measurements for the diagnosis of cholesteatoma. *Diagn Interv Radiol* 2017;**23**(4):300–6. https://doi.org/10.5152/dir.2017.16024.
16. Russo C, Elefante A, Di Lullo AM, *et al*. ADC benchmark range for correct diagnosis of primary and recurrent middle ear cholesteatoma. *BioMed Res Int* 2018;**2018**:1–6. https://doi.org/10.1155/2018/7945482.
17. Suzuki HSM, Yoshida T, Otake H, *et al*. Numerical assessment of cholesteatoma by signal intensity on non-EP-DWI and ADC maps. *Otol Neurotol* 2014;**35**(6):1007–10. https://doi.org/10.1097/MAO.0000000000000360.
18. Lingam RK, Nash R, Majithia A, *et al*. Non-echoplanar diffusion weighted imaging in the detection of post-operative middle ear cholesteatoma: navigating beyond the pitfalls to find the pearl. *Insights Imaging* 2016;**7**(5):669–78. https://doi.org/10.1007/s13244-016-0516-3.
19. Fukuda A, Morita S, Harada T, *et al*. Value of T1-weighted magnetic resonance imaging in cholesteatoma detection. *Otol Neurotol* 2017;**38**(10):1440–4. https://doi.org/10.1097/mao.0000000000001558.
20. Karandikar A, Loke SC, Goh J, *et al*. Evaluation of cholesteatoma: our experience with DW Propeller imaging. *Acta Radiol* 2015;**56**(9):1108–12. https://doi.org/10.1177/0284185114549568.